BINGO

a better future under CLIMATE CHANGE

BRINGING INNOVATION TO ONGOING WATER MANAGEMENT

D2.3

Definition of extremal circulation patterns, present climate

November 2016

www.projectbingo.eu

The BINGO project has received funding from the European Union's Horizon 2020 Research and Innovation programme, under the Grant Agreement number 641739.

,

Horizon 2020 Societal challenge 5:
Climate action, environment, resource
efficiency and raw materials

BINGO

Bringing INnovation to onGOing water management –
a better future under climate change

Grant Agreement n° 641739, Research and Innovation Action

Deliverable number:	**D2.3**
Deliverable name:	**Definition of extremal circulation patterns, present climate**
WP / WP number:	WP2: Climate predictions and downscaling to extreme weather
Delivery due date:	Project month 12 (29/06/2016)
Actual date of submission:	30/06/2016, re-submitted 14/11/2016.
Dissemination level:	Public
Lead beneficiary:	FUB
Responsible scientist/administrator:	Uwe Ulbrich, Henning Rust
Estimated effort (PM):	5PM
Contributor(s):	Christos Vagenas, Edmund Meredith, Agbeko Komlan Kpogo Nuwoklo, (FUB)
Estimated effort contributor(s) (PM):	4PM
Internal reviewer:	Suggested internal reviewers: Tim aus der Beek, Erle Kristvik

Changes with respect to the DoW
With justification if applicable

Dissemination and uptake
D2.3 – Definition of extremal circulation patterns, present climate.

Short Summary of results (<250 words)
This deliverable addresses the issue of identifying large scale atmospheric patterns with high probability of producing extreme precipitation events for the RS. The Wupper catchment, located in West Germany, has been used in this text to exemplify the approach followed in WP2. The methods used here combine the definition of weather types based on a sophisticated clustering algorithm (Simulated ANnealing and Diversified RAndomisation, SANDRA) and a regression approach based on a logistic model (special case of generalized linear models, GLM). This combination exploits the benefits of including highly non-linear drivers of extreme precipitation via a discrete set of weather types and the flexibility of a generalized linear model to include continuous variables such as convectively available potential energy (CAPE), relative humidity and wind speed.

This revised version of the deliverable report has been amended to (i) take account of the latest status of the availability of the high-resolution test-simulations for the Tagus research site (page 6), which are now fully available, and (ii) to clarify that the Cyprus research site employs the same methodology for the identification of extremal weather patterns as the other research sites (page 10), albeit with a slightly different modelling strategy (page 6).

Evidence of accomplishment
This report.

TABLE OF CONTENTS

1. INTRODUCTION

For the present deliverable, the linkage between extreme precipitation events and atmospheric patterns is investigated and established in the form of an identification algorithm based on a combination of weather typing and logistic regression. The question can be formulated as, “are there certain atmospheric situations which have high probability of producing extreme precipitation events and, as a result, floods?” If such extremal patterns can be identified from the large scale situations, the effort of high resolution dynamical downscaling of extreme precipitation events can be dramatically reduced and the available computing time can be used more efficiently.

This deliverable consists of two parts, (a) the high resolution dynamical downscaling of test episodes for all research sites which are meant to establish the chain from generating high resolution meteorological surface data to input data to hydrological models for each RS. This part is described in the subsequent Section 2. Part (b) of the deliverable is the identification of extremal episodes which is detailed in Sections 3 to 5. The aforementioned parts (a) and (b) have been amended in November 2016 to update the status of the availability of simulations for the Tagus research site (page 6), and to provide additional clarification on how the described methods are employed for the Cyprus research site (pages 6 and 10), respectively.

2. HIGH RESOLUTION SIMULATION OF EXTREME EPISODES

2.1 Theory and Methods

Extremal weather patterns and individual events of hydrological significance shall be identified from the 0.11° simulations carried out with the COSMO-CLM (CCLM) regional climate model, for each of the 6 research sites. These shall be subjected to more detailed analyses. In the case of extreme precipitation events, a phenomenon with high spatial variability, this involves further dynamic downscaling of the identified events up to a convection-permitting resolution of 0.02° (2.2 km). This provides a better representation of the dynamics driving any changes in hydrological extremes and hence a more detailed input for the hydrological models. In convection-permitting simulations, deep convective processes can be explicitly simulated by the model, where they have to be otherwise parametrized in lower-resolution simulations, i.e. our 0.11° CCLM integration. The further downscaling to convection-permitting resolution is a key step, as recent studies have shown that convection-permitting resolution is essential to accurately capture the response of convective precipitation extremes to climatic changes (Kendon et al. 2014, Ban et al. 2015), which can be highly nonlinear (Meredith et al. 2015).

The issue of spatial spin-up - meaning the distance from the lateral boundaries at which fine-scale features can be achieved - is an important consideration when designing regional downscaling experiments. For consistency, we intend to use a common domain for all high-resolution simulations at each research site. As the large-scale forcing behind individual extremes can come from any side of the domain, we centre our high-resolution domains over each research site and use a 201 x 201 grid, with 50 vertical levels. This allows at least 100 grid-lengths between the lateral boundaries and the centre of each research site. Brisson et al. (2015) investigated the impact of domain size on the simulation of precipitation in convection-permitting models, using a horizontal grid spacing of 3 km. They concluded that a spatial spin-up of at least 40 grid cells is necessary for the realistic simulation of precipitation patterns. For more detailed discussion of convection permitting modelling the reader is referred to Prein et al., 2015.

2.2 The simulations

With the aid of the questionnaire responses from each research site, one extreme precipitation event has been identified from the 0.11°-CCLM simulations for each site (excluding Cyprus), and has been further downscaled to 0.02° resolution (2.2 km) with the CCLM. The events for these test-simulations were subjectively identified from the 0.11° degree model output, based on the questionnaire descriptions of past extremes at each site and the 0.11° modeled precipitation.

As described in the DoW, for the case of Cyprus a different modelling strategy was followed. Since the Cyprus research site lies at the very edge of the EURO-CORDEX domain (that was used for the 0.11° degree CCLM simulations), sensitivity to the large-scale boundary conditions are considered by additional runs with the WRF model forced over a different domain. Other than this, the approach is analogous to that employed at the other sites.

The output variables are at an hourly frequency and have been made available for the same parameters as shown in Table 1, though there are obviously no daily min/max's provided. All data are available through the Freva DECO plugin, and are best accessed by selecting "test-events" in the experiment field and then the appropriate research site (i.e. Badalona, Bergen, Tagus, Veluwe, Wupper) in the product field.

Table 1 – BINGO Variables. *Time method refers to the highest frequency data; daily means are calculated by averaging the highest frequency data. Variable IDs for daily min/max are formed by appending either 'min' or 'max' to the variable ID, e.g. clt[min|max]. A "day" is defied as 24-hours from 00:00 UTC. All time-stamps in the output data are in UTC.

Variable Description	Variable ID	Frequency	Time Method*	Min/Max†
Total Cloud Fraction	clt	3-hr, day	Instantaneous	Daily
Near-Surface Relative Humidity	hurs	3-hr, day	Instantaneous	Daily
Near-Surface Specific Humidity	huss	3-hr, day	Instantaneous	Daily
Precipitation	pr	1-hr, 3-hr, day	Mean	Daily
Surface Air Pressure	ps	3-hr, day	Instantaneous	Daily
Sea Level Pressure	psl	3-hr, day	Instantaneous	Daily
Surface Downwelling Longwave Radiation	rlds	3-hr, day	Mean	Daily
Surface Downwelling Shortwave Radiation	rsds	3-hr, day	Mean	Daily
Near-Surface Wind Speed	sfcWind	3-hr, day	Instantaneous	Daily
Near-Surface Air Temperature	tas	3-hr, day	Instantaneous	Daily
Near-Surface Dew Point Temperature	tdps	3-hr, day	Instantaneous	Daily
Eastward Near-Surface Wind	uas	3-hr, day	Instantaneous	Daily
Northward Near-Surface Wind	vas	3-hr, day	Instantaneous	Daily

Project partners are asked to download the high-resolution test-simulations for their respective research sites and test the data on their hydrological models. Feedback should then be provided as soon as possible. The earlier feedback is received, the more likely that any concerns raised can be satisfactorily addressed. Feedback on the test simulations is best provided to Edmund Meredith (edmund.meredith@met.fu-berlin.de).

3. DATA AND REGION FOR DEFINING EXTREMAL EPISODES

Data from the ECMWF ERA-Interim daily database are used as input for the cluster and regression analyses. These data cover the period from 1979 to 2015 with a spatial resolution of 0.75º. Precipitation data are available through the EU WATCH (WATer and global CHange) Forcing Data Era Interim – WFDEI dataset (Weedon et al. 2014), covering the period from 1979 to 2013 on a grid resolution of 0.5º. Both datasets use a regular grid. The full list of the used data is presented in Table 2. These data are used for all six research sites of the BINGO project. Here, we detail the approach exemplarily for the German RS over the Wupper catchment. The grids of the different data sets used are depicted in Figure 1.

Table 2 – Used data description

Variable	Source	Time period	Grid resolution
Mean Sea Level Pressure	ERA-Interim	1979-2015	0.75º
Geopotential at 500 hPa	ERA -Interim	1979-2015	0.75º
Convective Available Potential Energy	ERA -Interim	1979-2015	0.75º
Relative Humidity at 1000 hPa	ERA -Interim	1979-2015	0.75º
Relative Humidity at 700 hPa	ERA -Interim	1979-2015	0.75º
Precipitable Water	ERA -Interim	1979-2015	0.75º
Vertical Velocity at 800 hPa	ERA -Interim	1979-2015	0.75º
Wind Speed at 700 hPa	ERA -Interim	1979-2015	0.75º
Wind Direction at 700 hPa	ERA -Interim	1979-2015	0.75º
Precipitation	WATCH	1979-2013	0.5º

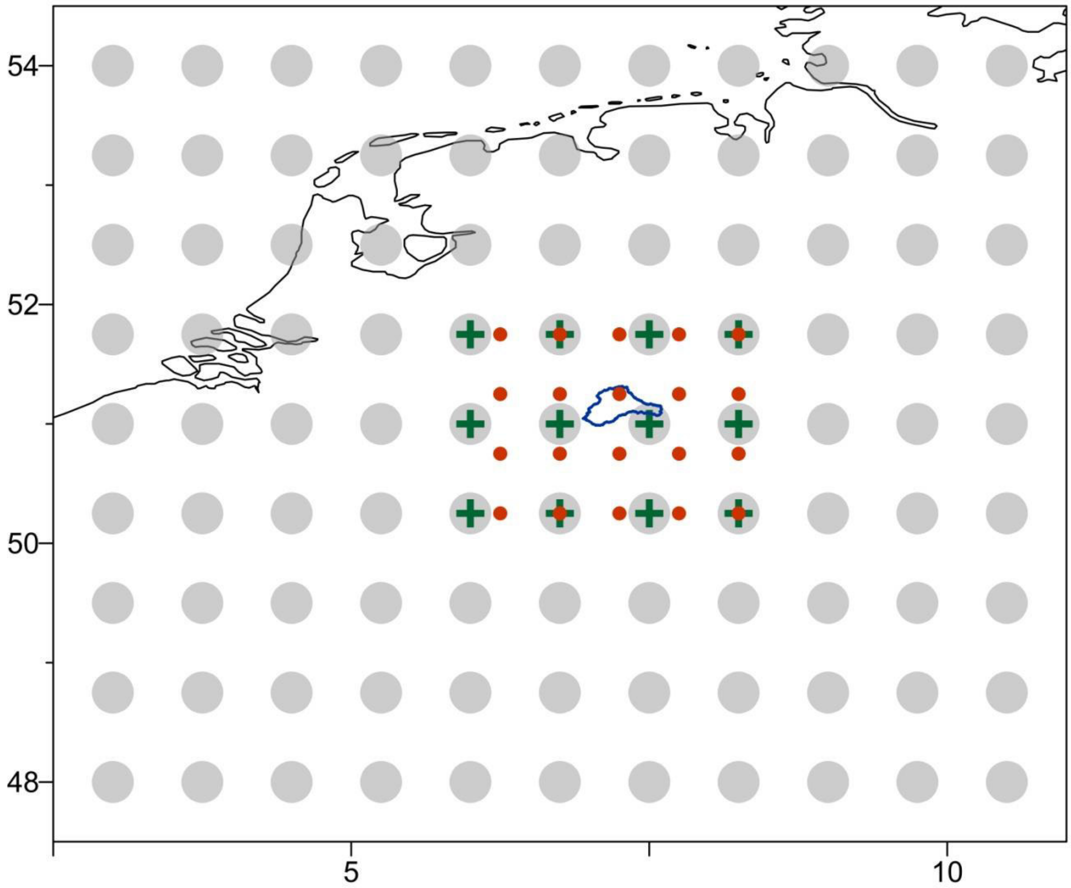

Figure 1 – Grid points around the Wupper catchment (blue line). Large gray circles for ERA-interim box2, green crosses for ERA-Interim box3 and small red circles for WATCH.

4. METHODOLOGY

3.1 Cluster analysis

The methodology described below for identifying extremal patterns will be used for all six research sites, i.e. including Cyprus.

Cluster analysis is applied in order to create a discrete set of data (weather types), whose relationships (dis-/similarities) are not known beforehand. Also, not known is the ideal number of these clusters (weather types) that will best summarize and separate the original data. The end product of a cluster analysis is a discrete set which have some physical basis and give information and insight about the data structure that would had been difficult to be identified without the application of such an exploratory method (Hastie et al. 2009, Wilks 2011).

The objects inside each cluster should have the best possible similarity, while between the different clusters the highest dissimilarity should be exhibited. This is achieved by an iterative proccess of rearranging objects into different clusters in every step until there is no more room for improvement by further rearrangements. Then it is said that a “local optimum” is reached, although there is no guarantee that it is close to the ideal “global optimum” (the best possible solution) (Philipp et al. 2007).

Simulated ANnealing and Diversified RAndomization cluster analysis (SANDRA) is a relatively new cluster analysis method, that have been applied in meteorological and climatological practices mostly during the last decade. SANDRA cluster analysis can be applied through the open source cost733class software package (cost733.geo.uni-augsburg.de/cost733class-1.2), which has been developed to create, compare, visualize and evaluate weather and circulation type classifications with in the EU COST Action 733.

SANDRA has been developed in order to deal with some shortcomings of the more traditional K-means cluster analysis. These include a) a cluster generation which is biased by the starting partitions and b) the dependence of the ordering of checks and reassignments. SANDRA cluster analysis overcomes these problems, mainly because it is not bound to the concept of irreversible paths throughout the optimization process. This means that it does not converge to a local optimum that cannot be left anymore but allows an object to leave its temporarily assigned cluster at any stage of the proccess (with a specific probability), even if this step does not immediately improve the result towards the local optimum (Philipp et al. 2007). Also, its much better stability over K-means for large datasets is addressed by Huth et al., 2008. So, by application of the SANDRA cluster analysis, the probability of reaching the global maximum is significantly increased, while the probability of convergence to a local minimum is reduced.

3.2 Logistic regression model for exceedance probabilities

It is meaningful to include the influence of weather types defined, e.g. by sea level pressure or geopotential heights, as discrete classes to account for their strongly non linear influence on precipitation extremes. These weather types (or clusters) are obtained as described in Sect. 3.1. A large part of the main influence of other variables, such as convective available potential energy, precipitable water, and relative humidity, might well be captured with linear models. To this end, we set up a logistic regression model (a special case of a generalized linear model (McCullagh and Nelder 1989, Rust 2013) for the probability of daily precipitation intensities at a grid point close to the research site exceeding a threshold additionally to the partition of weather states into clusters.

The result of such a model is a probability for a threshold excess given the values of a set of predictor variables, e.g. from a GCM simulation. We then use days with high probability of threshold exceedance as basis for selecting extremal episodes to be dynamically downscaled to a high resolution with an RCM.

Logistic regression models are extensively described in (McCullagh and Nelder 1989, Wilks 2011, Wood 2006) and have been used for modelling precipitation occurrence probabilities (exceeding the threshold 0.1 mm/day) in, e.g., Rust 2013. The theory of GLMs and the special case of logistic regression is basic textbook material and thus not covered here.

However, the process of building such a model is an intellectual challenge and involves some ideas of what are important drivers (predictors) for extreme precipitation occurence (predictant). From personal experience and literature reviews we chose to screen the following variables as potential continuous predictors from the coarse scale for the model:

- convective available potential energy (CAPE), daily mean and max,
- precipitable water (PWAT), daily mean and max,
- horizontal wind speed at 700 hPa (Spd700), daily mean and max,

- horizontal wind direction at 700 hPa (Dir700), daily mean,
- vertical wind speed at 800 hPa (W800), daily mean and max, and
- relative humidity at 700, 850 and 1000 hPa (RH700, RH850, RH1000, daily mean and max).

5. DESCRIPTION OF WORK

4.1 Extreme events

The current aproach for extreme precipitation days includes the WATCH grid points that fall into the catchment of interest and also the grid points surrounding it. The idea is that with similar atmospheric conditions, exteme precipitation events may happen inside the catchment, in the vicinity of the catchment, or in both, during its developement. So, looking into precipitation that occurs outside the strict limits of the catchment ensures that no extreme events will be missed. For a given threshold *u* of daily precipitation, if any of the grid points exceed this threshold then the day is addressed as an extreme precipitation day.

For the Wupper catcment, strong seasonality is observed in the daily precipitation amounts. Figure 2 shows the frequency of daily precipitation amounts over 10 (left) and 21 mm (right), respectively. The values represent the central grid point that falls into the catchment. It can be seen that for days over 21 mm of rainfall (about the 97.5th percentile of rainy days) the three highest frequency months fall into three different seasons. It is reasonable to perform the subsequent cluster and regression analyses on a seasonal basis, in order to explore the different atmospheric states that produce heavy rainfall events.

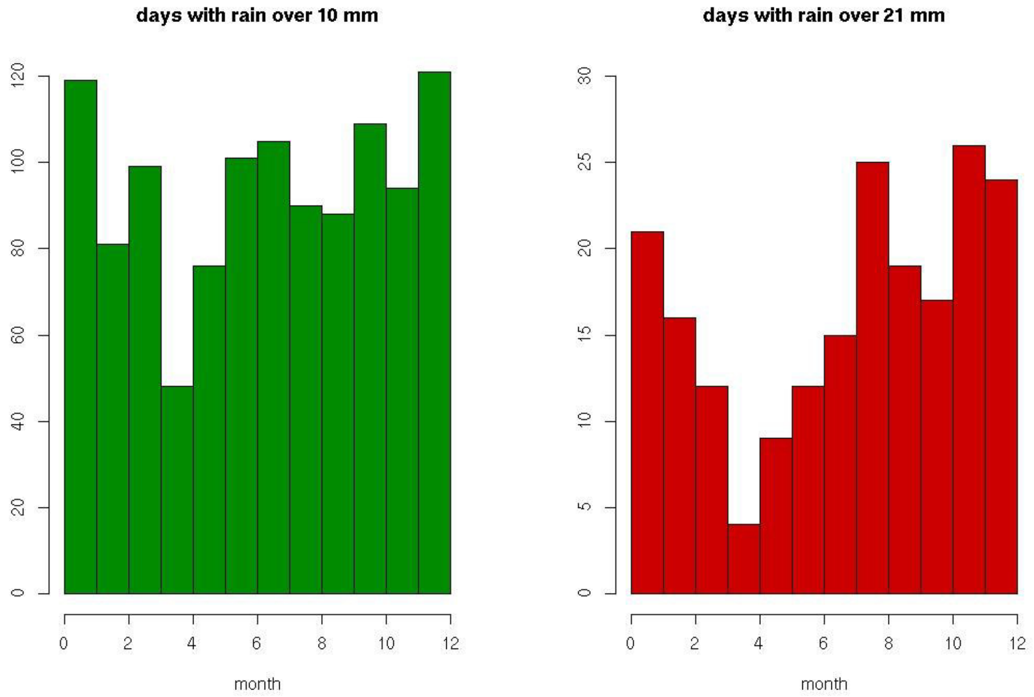

Figure 2 – Monthly frequencies for daily precipitation over 10 mm (left) and 21 mm (right) for the period 1979-2013 in the Wupper catchment.

4.2 Cluster analysis

In order to perform the cluster analysis for circulation patterns, a domain of study must be defined. At first three different domains were tested. A large domain, referred to as box1, covering most of the European region, approximately 20° south, east and north and 25° west of the center of the Wupper catchment (not shown). Two smaller domains were also tested (Fig. 1), termed box2 and box3, which, ultimately, have been found to produce better results than box1.

For the scope of the present deliverable, the datasets used consist of time dependent spatial fields of various continuous meteorological variables, e.g. mean sea level pressure (SLP, to be used for the clustering), convectively available potential energy (at a grid point to be used in the regression), and their mean or maximum daily values. The variables are spatially distributed over a number of grid points, so there are numerous daily values in each object. As the cluster analysis is applied, each day is assigned into a cluster, of the predefined total cluster number (trials from 3 to 45 clusters by steps of 3), alongside with days of similar conditions.

After many reassignments and rearrangements the final result should be well defined pressure patterns. Ideally, there would be separate clusters associated with high probability of extreme precipitation and clusters with very low or zero probability of extreme precipitation. Examples for SLP and Z500 are presented in Figures 3 and 4.

In order to account for seasonality of the various atmospheric patterns and states, the cluster analyses were applied to seasonal data sets. The traditional three month separation was used: DJF, MAM, JJA and SON. By several trials it has been found that variables like SLP and Z500 produce better results for the box2 domain than the domains of boxes 1 and 3. Other variables, like relative humidity and CAPE seem to have a better response in box3.

For the precipitation data, gridded daily sums of the WATCH dataset are used. In order to explore the relationship of the clustering result with extreme precipitation, the different thresholds *u* for daily precipitation amount are tested for each grid point (in a future stage Extreme Value Theory – EVS techniques will be applied for determining the extreme threshold values).

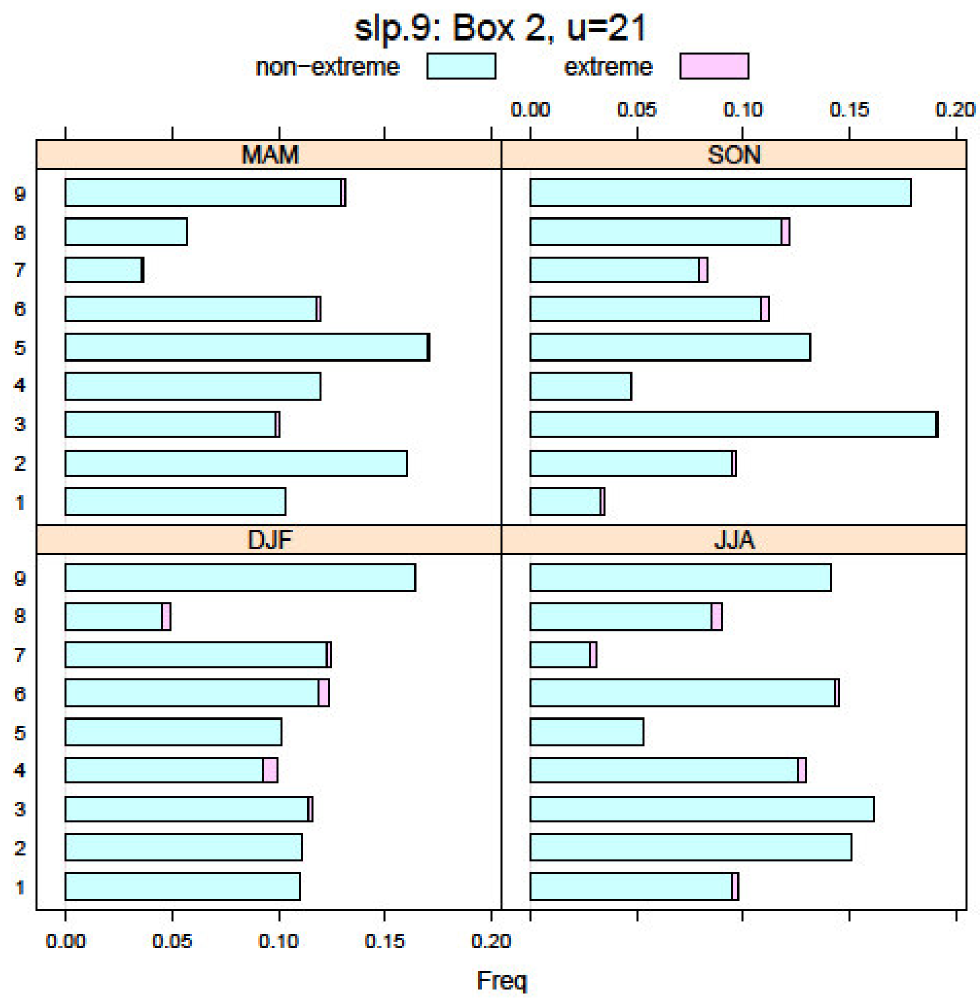

Figure 3 – SLP seasonal results for 9 clusters. Bars indicate occurrence frequency for each cluster (x axis) with light blue and pink colors representing days below and above the 21 mm per day precipitation threshold, respectively.

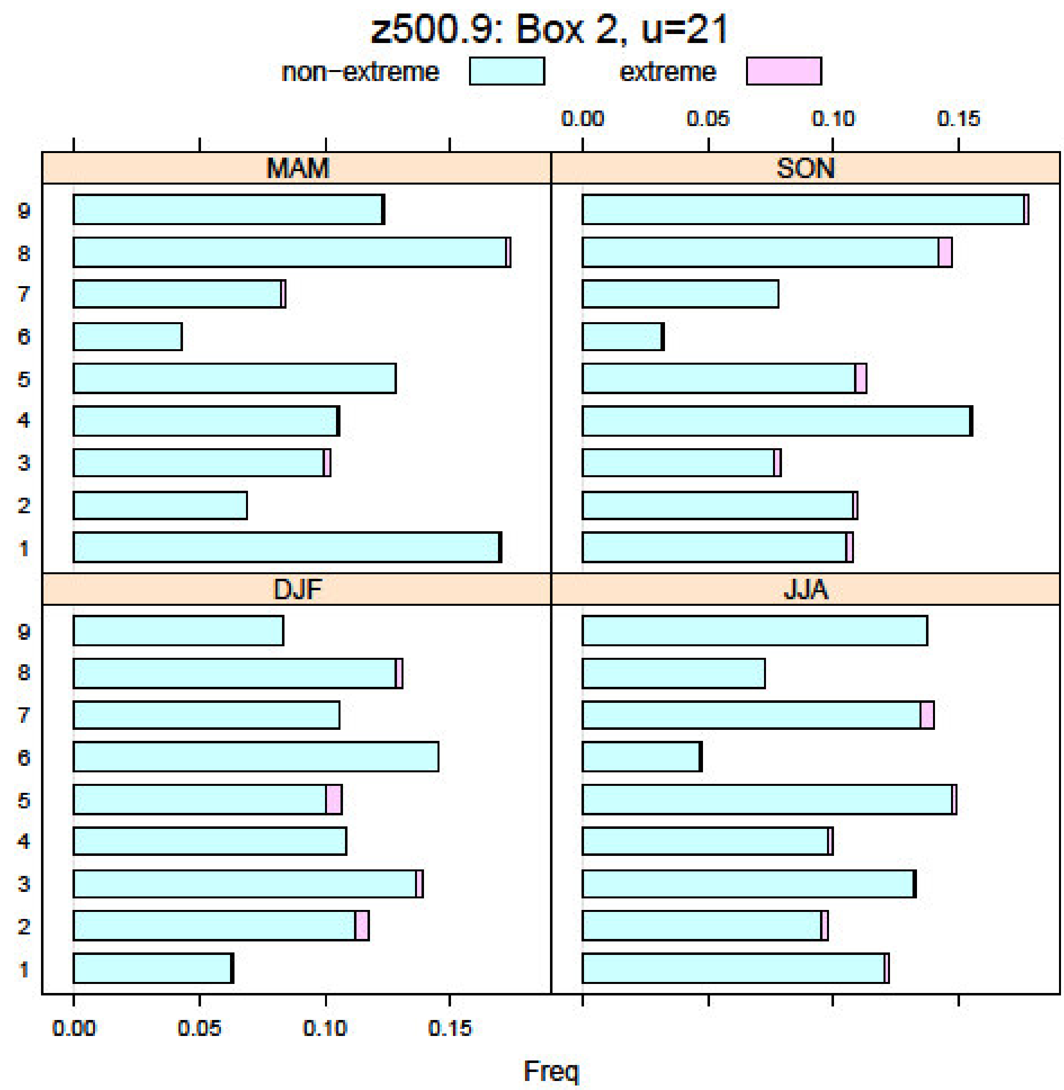

Figure 4 – As in Fig. 2 but for Z500.

4.3 Logistic regression model for exceedance probabilities

Scatterplots as in Fig. 5 are used to screen the predictors and, if applicable, decide on a predictor transformation. The influence of CAPE can be better captured if a static logarithmic transformation is applied, $log(1 + cape)$. The logarithm leads to reduced influence of very high values and the addition of 1 ensures that a CAPE of 0 is mapped onto 0 after applying the logarithm. The influence of CAPE is clearly stronger in summer than in winter, whereas wind speed is more effective in winter. Figure 6 shows the influence of relative humidity (and precipitable water) at various levels. Whereas in summer the full range of relative humidity is occupied with precipitation events, only a small range is occupied in winter.

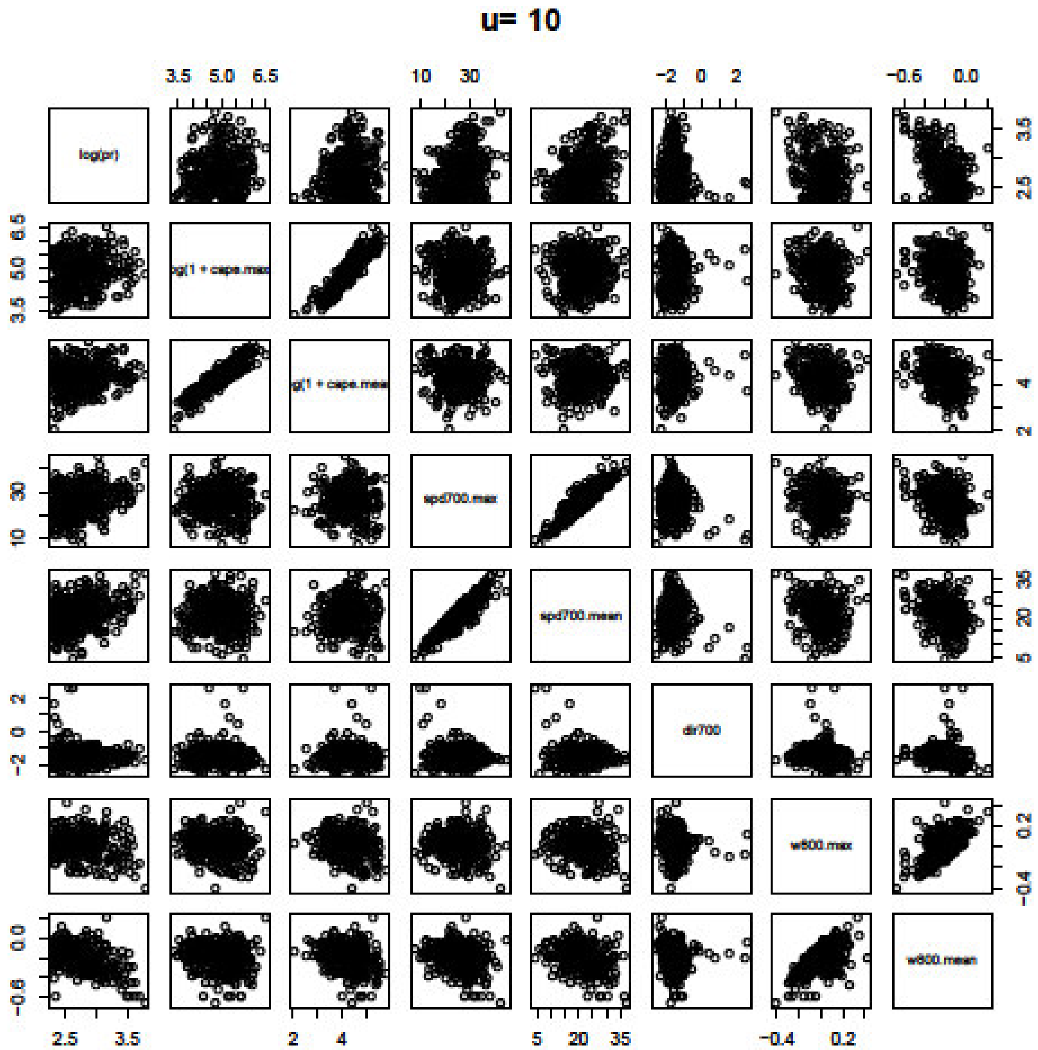

Figure 5 – Scatterplots of transformed CAPE and vertical and horizontal winds against precipitation over 10 mm to screen predictor influence.

While a first idea can be obtained from the scatterplots, predictor selection is the standard procedure in statistical modelling. Here, we start with a reasonable numer of weather types (6 and 9) and a small set of exceedance thresholds *u* (u=10,15,20), and perform an automated predictor selection. To this end, we set up a large model inlcuding all predictors and use a stepwise regression approach, with forward and backward selection based on the Akaike information criterion (AIC) (Wilks 2011). The resulting model contains the following predictors:

- log(1+CAPE.max)
- log(1+CAPE.max):W800.mean (interaction between vertical velocity and CAPE)
- PWAT.max

- PWAT.max:W800.max (interaction between precipitable water and vertical velocity)
- RH700.max
- RH1000.mean
- Spd700.mean

The regression model is conditioned on the season (DJF, MAM, JJA, SON) and the weather types. One can think of a separate regression model for each season and each weather type.

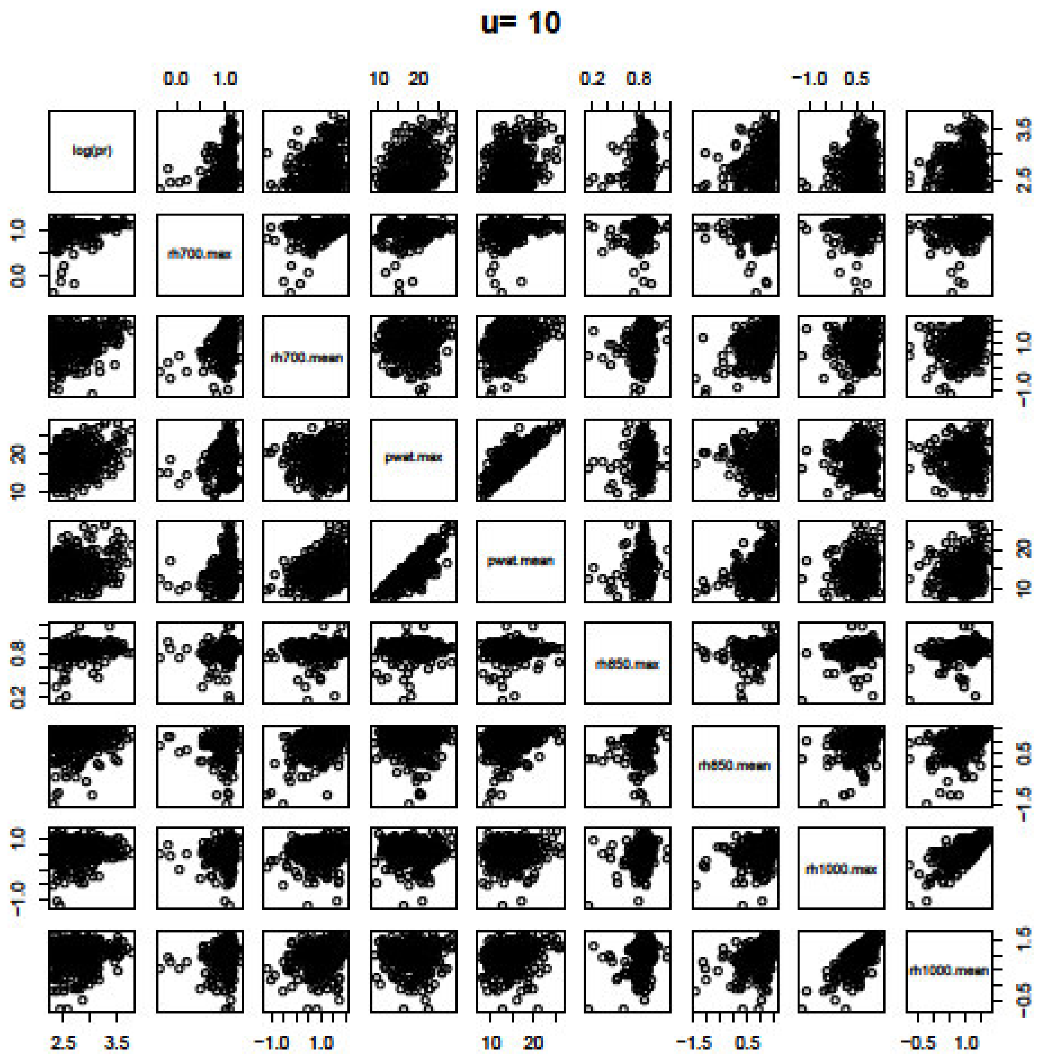

Figure 6 – As Fig. 5 but for relative humidity and perceptible water.

The performance of the model is now evaluated in a 7-fold cross validation experiment (Davison 1997) excluding a consecutive set of 5 years from the data set to estimate model parameters and then use these 5 years to validate the model's prediction for this period.

As we have a probabilistic forecast from the model, we set a probability threshold for which we consider the forecast as an event, e.g. for $p > 0.5$, and compare it with the observed data in the validation data set. This comparison is done for various thresholds p. We are now in the setting of comparing a binary forecast (0,1) to binary observations (non-extreme/extreme precip). For this setting, classical verification scores are the probability of detection (POD) and the false alarm rate (FAR) (Wilks 2011). Additionally, we calculate a fraction of days with an extreme event forecast. This number will be an estimate for the maximum days to be dynamically downscaled.

These three scores (POD, FAR, frac.sim) are obtained from an out-of-sample experiment and are thus a reliable measure for the number of events we might miss and the fraction of positive forecast which are likely to be extreme. We now obtain these scores for various maximum numbers of weather types (clusters, Ncl) and various thresholds *u* and compare these scores. Figures 7-15 show the result for 3, 6 and 9 clusters per season and thresholds of *u*=5, 15, and 21.

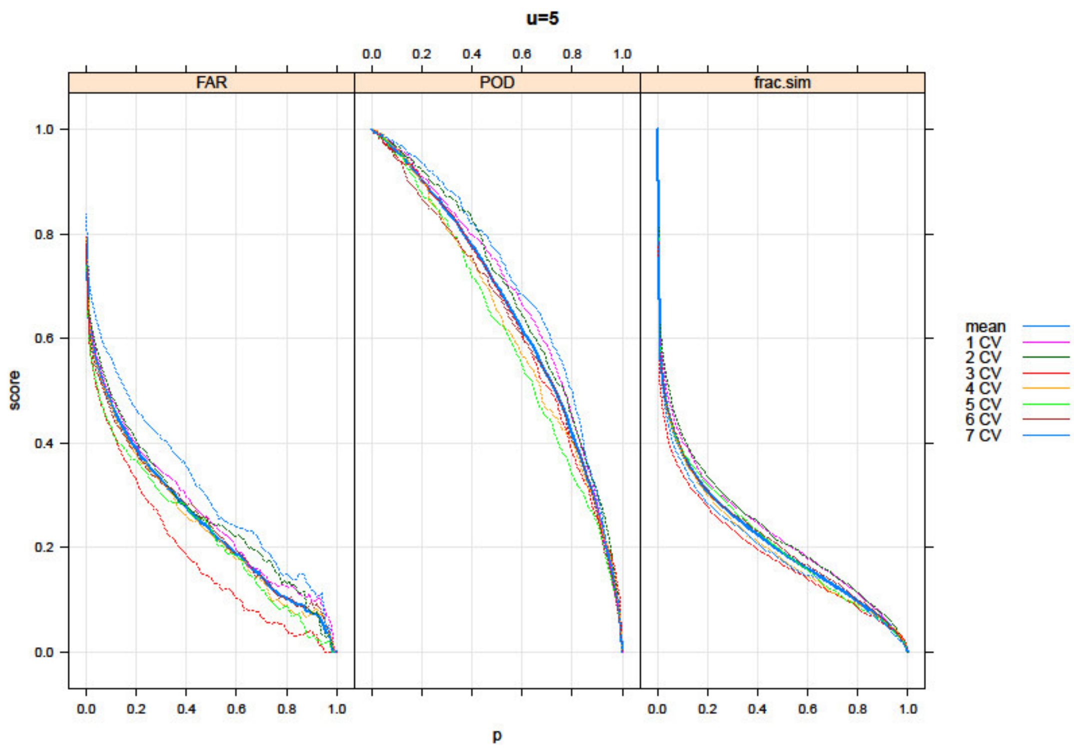

Figure 7 – False alarm rate (FAR, left) probability of detection (POD, middle) and fraction of days to simulate (frac.sim, right) for the logistic regression model with the above mentioned predictors for a threshold of 5 mm and 3 weather types.

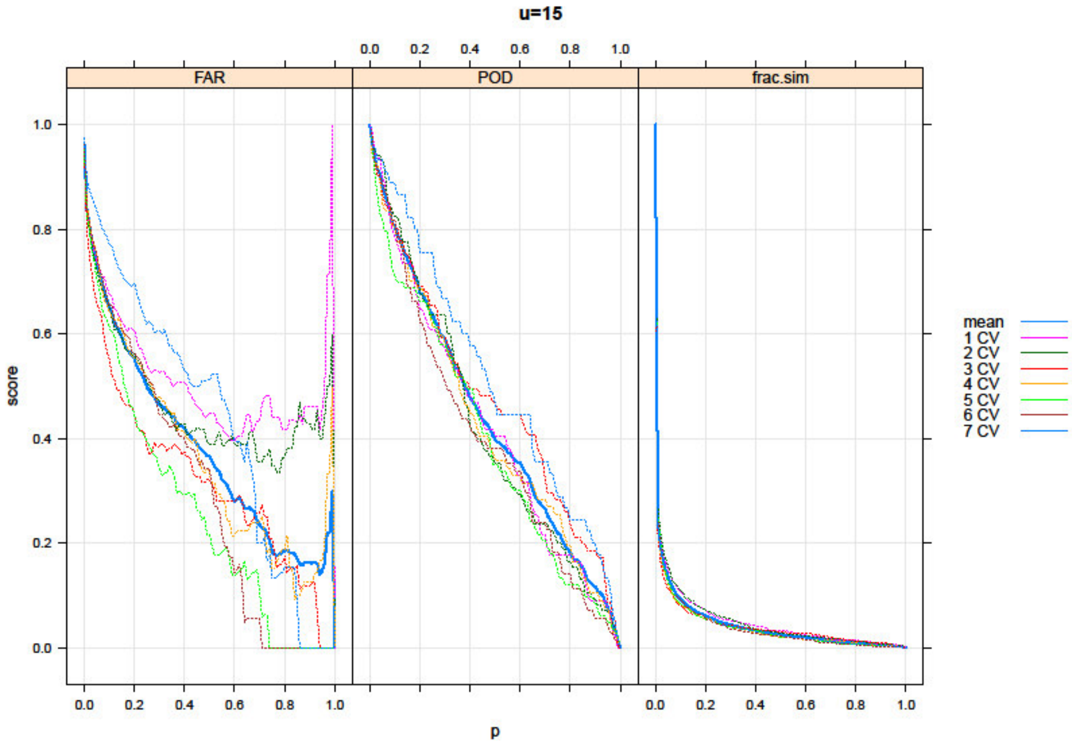

Figure 8 – Same as Fig. 7 but for a threshold of 15 mm.

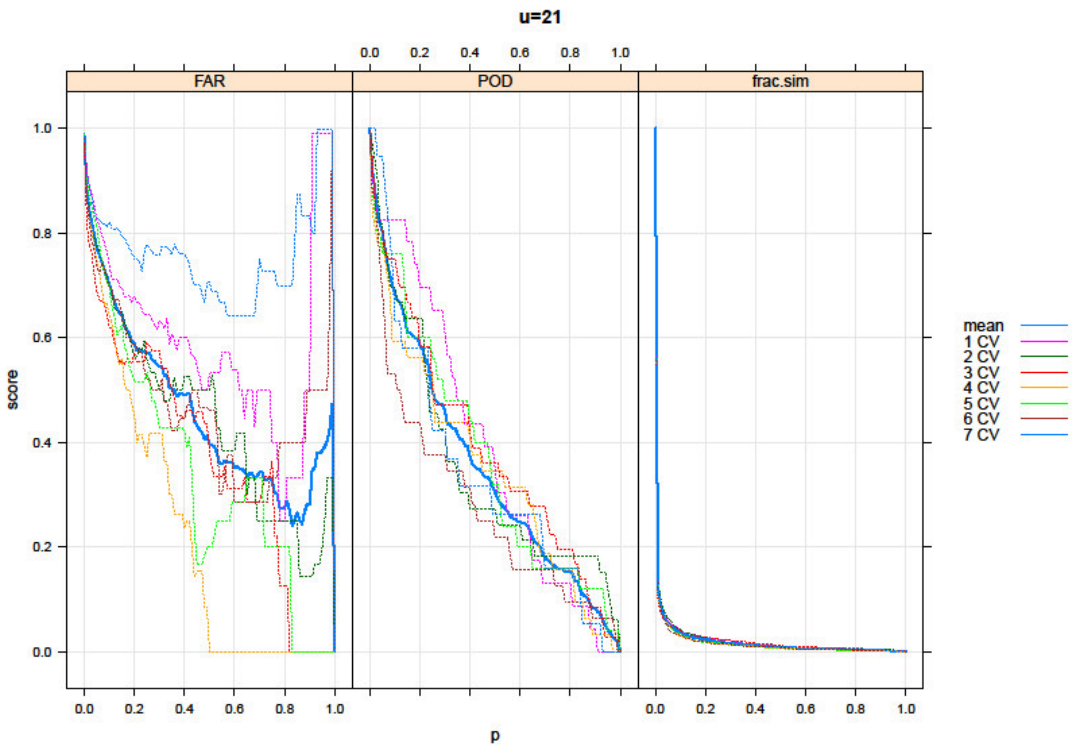

Figure 9 – Same as Fig. 7 but for a threshold of 21 mm.

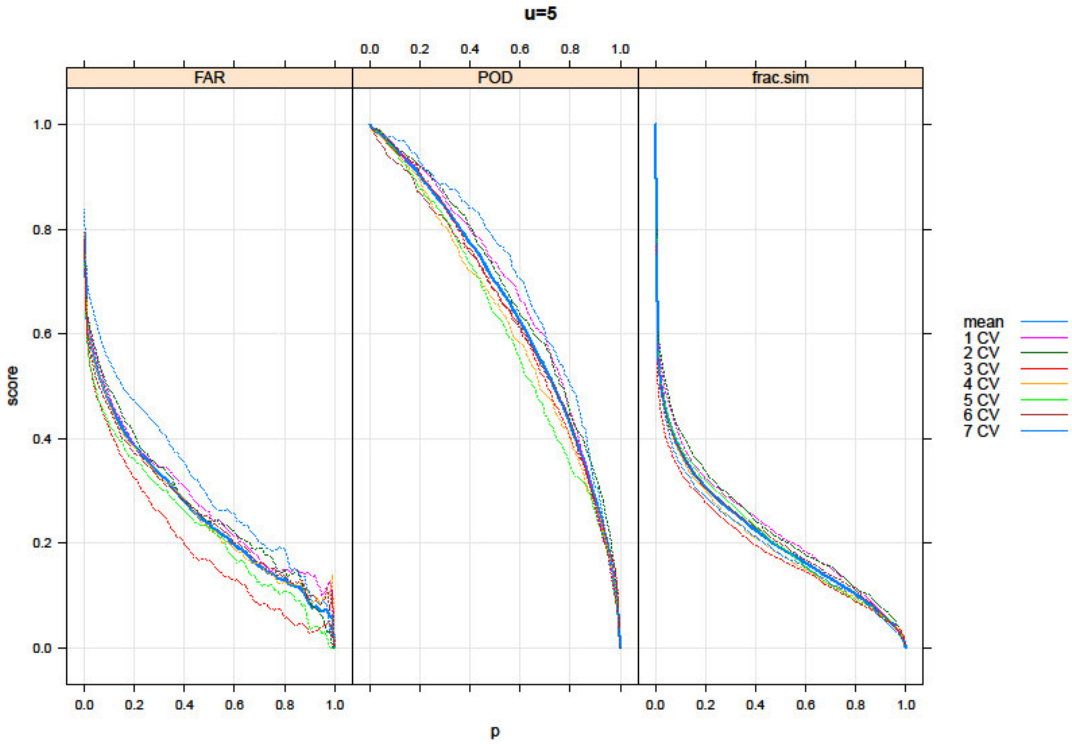

Figure 10 – Same as Fig. 7 but for 6 weather types and a threshold of 5 mm.

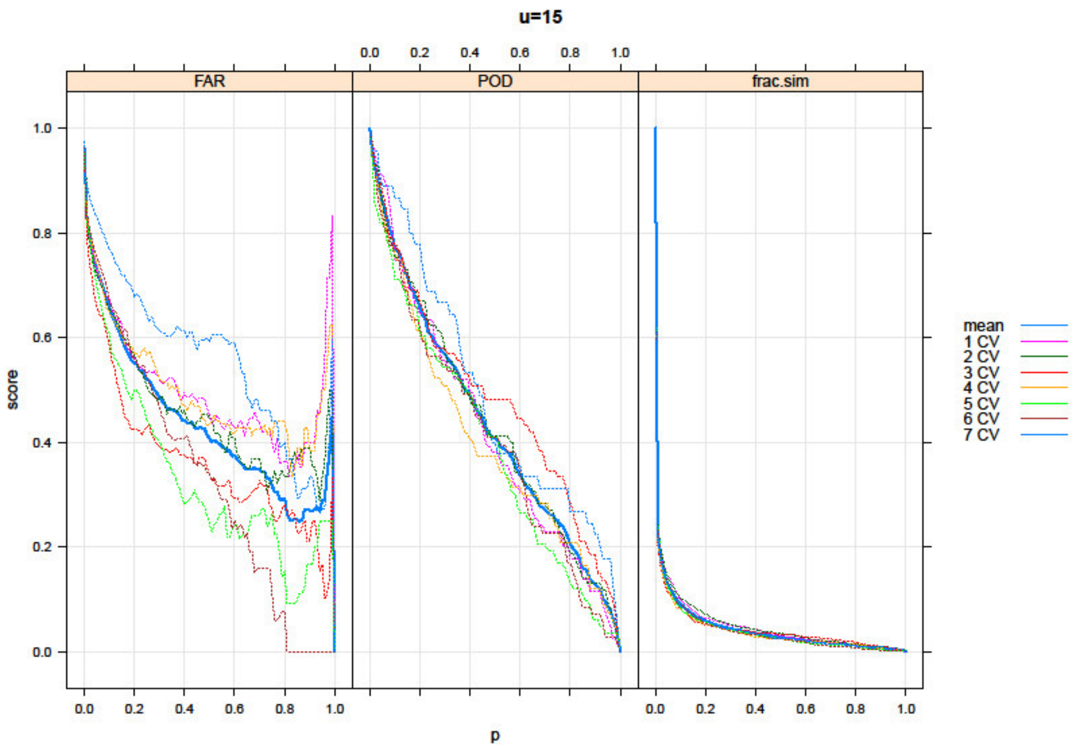

Figure 11 – Same as Fig. 10 but for a threshold of 15 mm

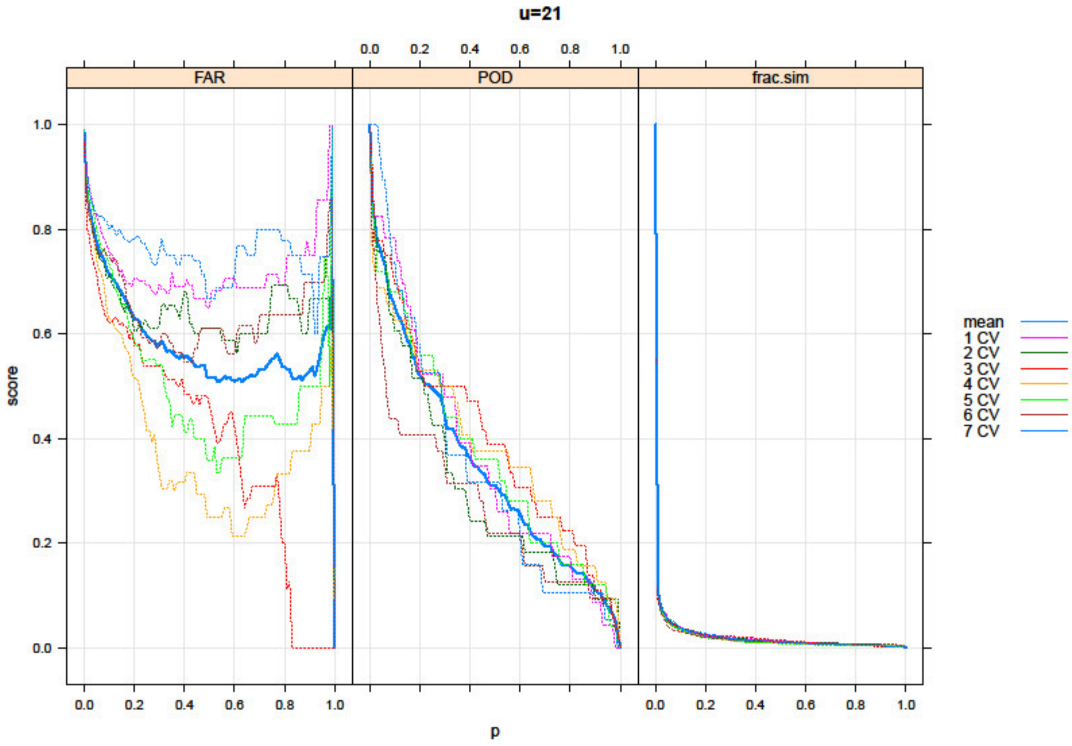

Figure 12 – Same as Fig. 10 but for a threshold of 21 mm.

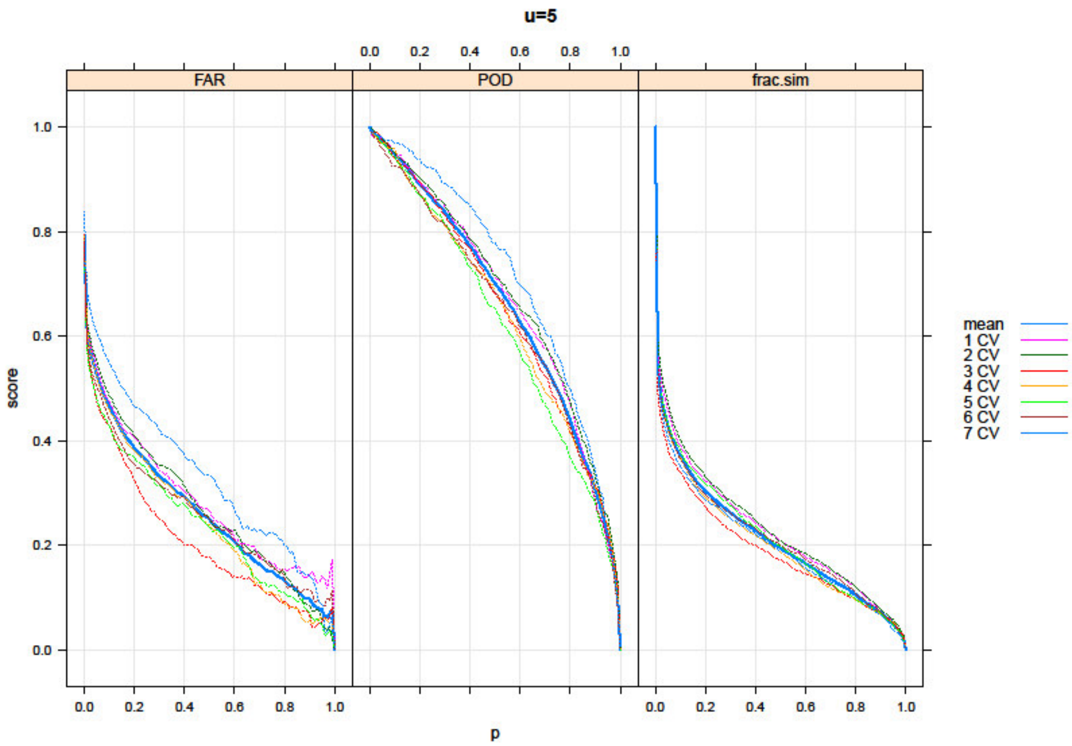

Figure 13 – Same as Fig. 7 but for 9 weather types and a threshold of 5 mm.

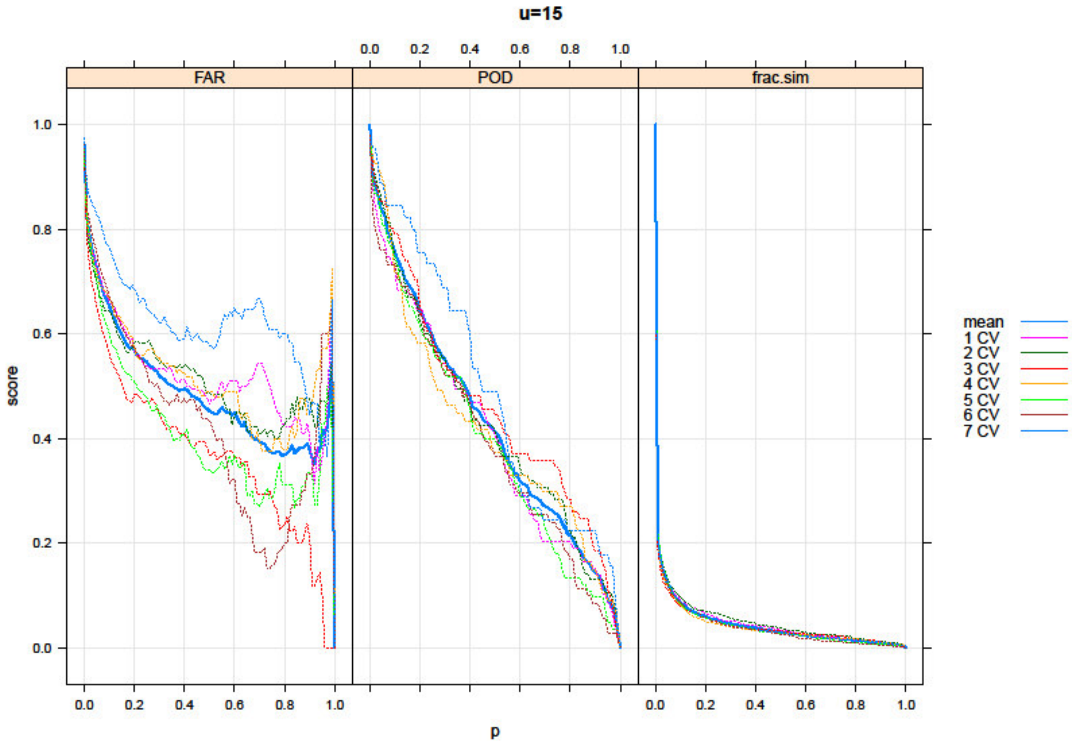

Figure 14 – Same as Fig. 13 but for a threshold of 15 mm.

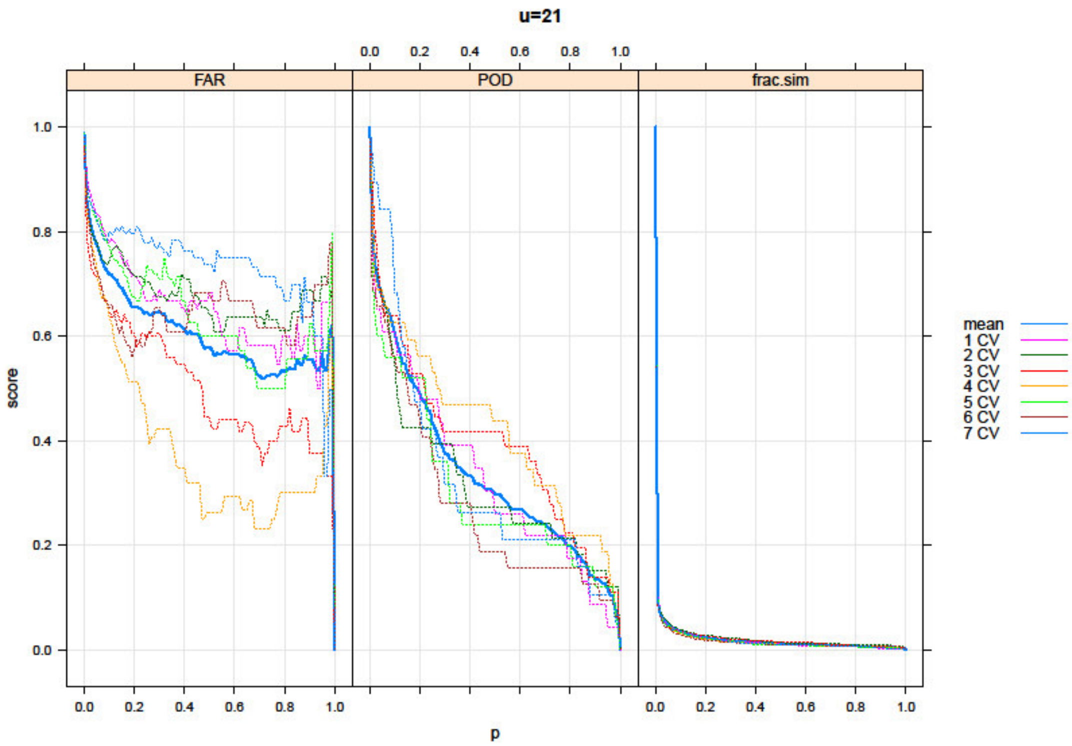

Figure 15 – Same as Fig. 13 but for a threshold of 21 mm.

The optimal compromise betwen fraction of days to simulate and an acceptable POD is obtained for 3 weather types based on SLP (Z500 has been tested but results are not shown) and a threshold of u=20 (Fig. 16). A probability threshold of p=0.1 ensures a POD of about 80% and a fraction of days to simulate below 10%. For the total time period used here (1979-2013) period, the extremal episodes cover about 4% of the total days.

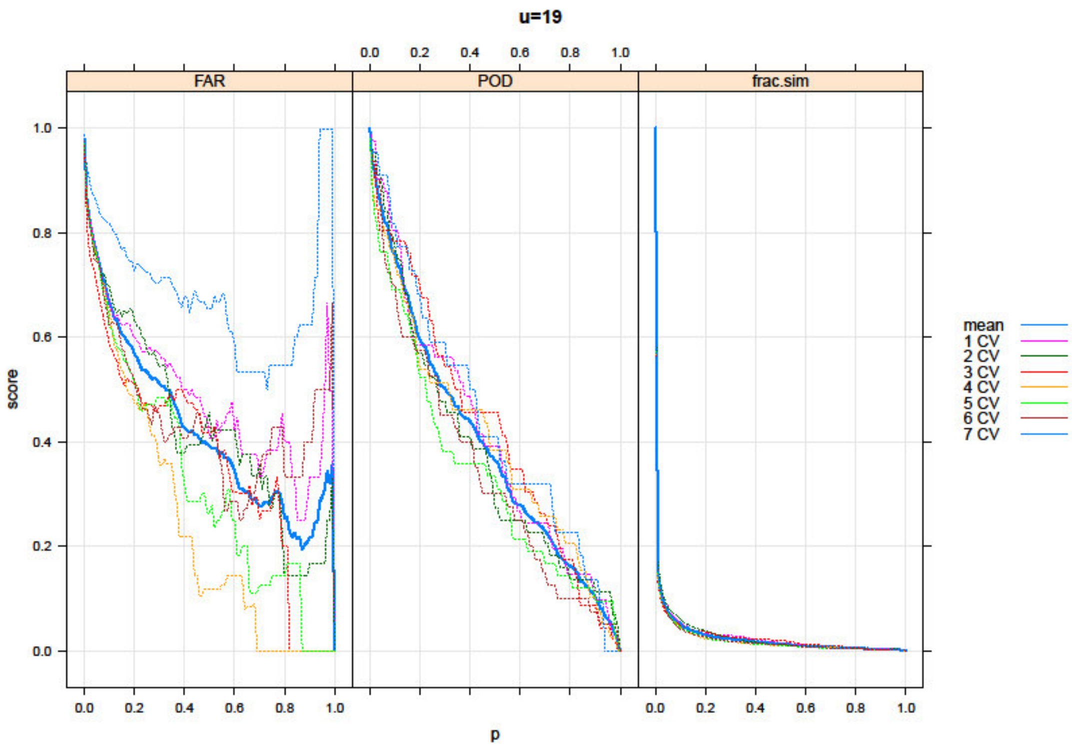

Figure 16 – Same as Fig. 7 but for 3 weather types and a threshold of 20mm.

Figures 17, 18 and 19 shows exemplarily the episode for the Wupper catchment for the years 2007, 2008, and 2013, respectively. These years have been communicated by the Wupperverband to contain recent extreme events (marked in cyan). While in 2007 and 2013 these events are well captured by the extremal episodes, the 2008 event is not well captured. As the reported 2008 event is not present in the WATCH data set which we used to define the episodes, it is plausible that it will not be detected by the algorithm presented here. This suggest to refine the definition based on local RS data instead of the global WATCH product. However, as the model is set up, this can be done quickly as soon as the RS have provided the local data.

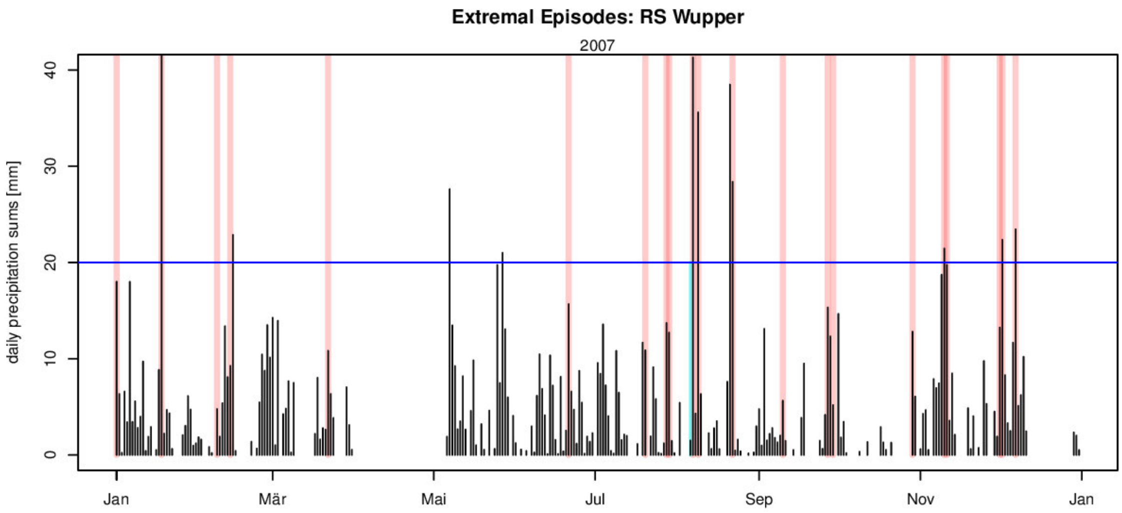

Figure 17 – Precipitation time series for the Wupper research site based on WATCH (black) with extremal episodes defined here (red) for the year 2007.

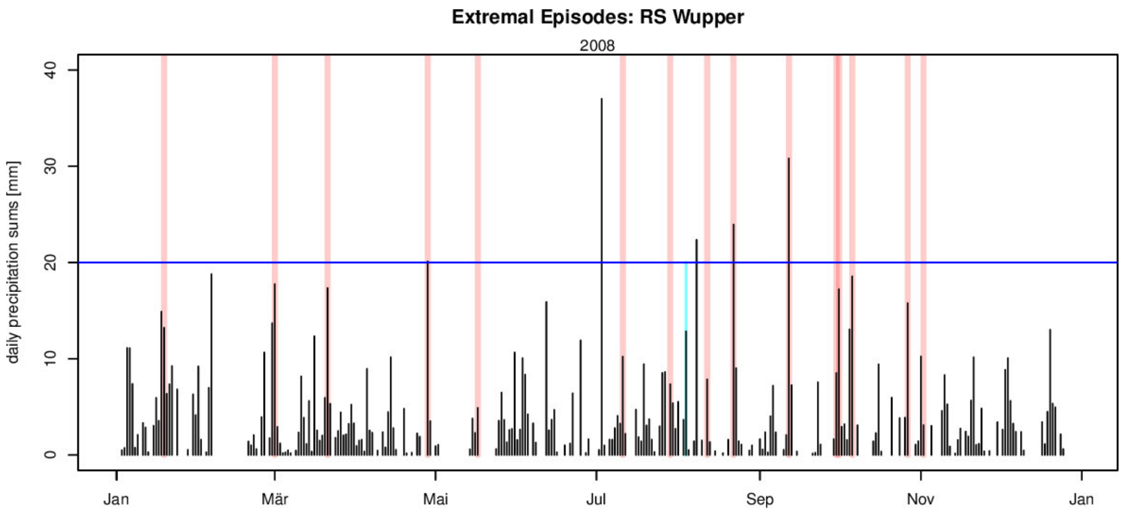

Figure 18 – Same as Fig. 17 but for the year 2008.

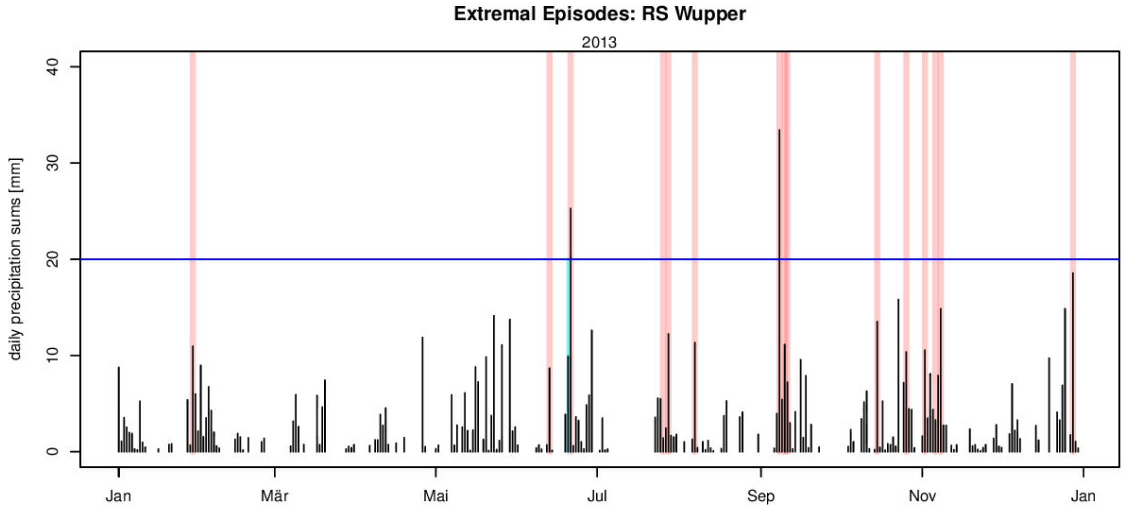

Figure 19 – Same as Fig. 17 but for the year 2013.

5. CONCLUSIONS AND DISCUSSION

The identification algorithm set up here combines the advantages of clustering approaches and generalized regression models; strongly non-linear drivers of extreme precipitation, such as surface pressure patterns are included via a discrete set of weather types (clusters). Within each weather type, the dependence on continuous variables such as CAPE, precipitable water, relative humidity or wind speed are capture with linear models. As we are interested only in situations with precipitation over a certain threshold, we model the probability of the daily precipitation sum exceeding this threshold by means of logistic regression. This approach to the problem is less challenging than a traditionall modelling of intensities would be and thus more likely to succeed.

We ended up with a relatively simple model including 3 weather types and a very reasonable number of continuous covariates (CAPE, vertical velocity, precipitable water, relative humidity and wind speed). For the RS Wupper, we find a very good agreement of the extremal episodes with the extremes present in WATCH. We do find also several extremal episodes which do not correspond with a WATCH extreme. These atmospheric situations however prone to yield extremes, i.e. they are such that they could have led to extreme rainfall at the RS but as precipitation is highly variable in space, the event has missed the site and probably happend close to it (see test event for the Wupper). As these situation can in deed also develop to an extreme at the RS under slightly modified conditions it is meaningful to include them into the set of episodes to be downscaled with the RCM where they possibly might develop into an extreme at the research site, while another one might not.

We thus finally have means to define a meaning canon of episodes for high resolution downscaling and have lowered the computational burden to a feasible extent.

GLOSSARY

CAPE	convective available potential energy
CLM	climate limited-area model
COSMO	consortium for small-scale modeling
DECO	data extraction and conversion
ECMWF	european centre for medium-range weather forecasts
ERA	european reanalysis
FAR	alse alarm rate
frac.sim	fraction of days to simulate
Freva	Freie Universität Berlin evaluation framework for earth system science
POD	probability of detection
PWAT	precipitable water
RHxxx	relative humidity at xxx hPa
SLP	mean sea level pressure
Wxxx	vertical velocity at xxx hPa
WATCH	water and global change
Zxxx	geopotential at xxx hPa

BIBLIOGRAPHY

Ban N., Schmidli J., Schaer C., 2015. Heavy precipitation in a changing climate. Does short-term summer precipitation increase faster? *Geophysical Research Letters*, 42, 1165-1172.

Brisson E., Demuzere M., van Lipzig N.PM., 2015. Modelling strategies for performing convection-permitting climate simulations. *Meteorologische Zeitschrift*.

Davison A.C., Hinkley D.V., 1997. Bootstrap methods and their application. *Cambridge University Press*, 582 pp.

Hastie T., Tibshira R., Friedman J., 2009., The elements of statistical learning: data mining, inference, and prediction, 2nd ed. *Springer*, 745 pp.

Huth R., Beck C., Philipp A., Demuzere M., Unstrnul Z., Cahynova M., Kysely J., Tveito O.E., 2008. Classifications of atmospheric circulation patterns: recent advances and applications. *Ann. N.Y. Acad. Sci.*, 1146, 105-152. doi:10.1196/annals.1446.019

Kendon E.J., Roberts N.M., Fowler H.J., Roberts M.J., Chan S.C., Senior C.A., 2014. Heavier summer downpours with climate change revealed by weather forecast resolution model. *Nature Climate Change*, 4, 570-576

McCullagh P., Nelder J.A., 1989. Generalized linear models, 2nd ed. *Chapman and Hall/CRC*, 532 pp.

Meredith E.P., Semenov V.A., Maraun D., Park W., Chernokulsky A.V., 2015. Crucial role of Black Sea warming in amplifying the 2012 krymsk precipitation extreme. *Nature Geoscience*.

Philipp A., Della-Marta P.M., Jacobeit J., Fereday D.R., Jones P.D., Moberg A., Wanner H., 2007. Long-term variability of daily north Atlantic-European pressure patterns since 1850 classified by simulated annealing clustering. *Journal of Climate*, 20, 4065-4095. doi:10.1175/JCLI4175.1

Prein A.F., Laughaus W., Fosser G., Ferrone A., Ban N., Goergen K., Keller M., Tolle M., Gutjahr O., Feser F.., et al., 2015. A review on regional convection-permitting climate modelling: Demonstrations, prospects, and challenges. *Reviews of Geophysics*, 53, 3262-3267.

Rust H., Vrac M., Sultan b., Lengaigne M., 2013. Mapping Weather-Type Influence on Senegal Precipitation Based on a Spatial-Temporal Statistical Model. *Journal of Climate*, 26, 8189-8209. doi:10.1175/JCLI-D-12-00302.1

Weedon G.P., Balsamo G., Bellouin N., Gomes S., Best M.J. and Viterbo P., 2014. The WFDEI meteorological forcing data set: WATCH Forcing Data methodology applied to ERA-Interim reanalysis data. *Water Resources Research*, 50. doi:10.1002/2014WR015638

Wilks, D. S., 2011. *Statistical* Methods in the Atmospheric Sciences, 3rd ed. *Academic Press*, 676 pp.

Wood S., 2006. Generalized additive models: an introduction with R. *Chapman and Hall/CRC*, 392 pp.